Available online at www.sciencedirect.com
ScienceDirect
Ceramics International 37 (2011) 3055–3062
CERAMICS INTERNATIONAL
www.elsevier.com/locate/ceramint

Oxidation resistance of multi-walled carbon nanotubes coated with polycarbosilane-derived SiC_xO_y ceramic

Ming Luo *, Yawei Li, Shengli Jin, Shaobai Sang, Lei Zhao

The Key State Laboratory Breeding Base of Refractories and Ceramics, Wuhan University of Science and Technology, Wuhan 430081, PR China

Received 14 March 2011; received in revised form 6 May 2011; accepted 9 May 2011
Available online 14 May 2011

Abstract

Multi-walled carbon nanotubes (MWCNTs) have been successfully coated with a thin SiC_xO_y coating when polycarbosilane (PCS) was used as precursor and pyrolyzed in a coke bed. Meanwhile, effect of PCS concentration on oxidation resistance of the coated MWCNTs is studied. The results showed that the pyrolysis products of PCS were composed of amorphous SiC_xO_y as the main phase, together with β-SiC and SiO_2 as the minor phases whose amount increased a little with the increase of temperature from 1000 °C to 1500 °C. The thickness of SiC_xO_y coating on the surface of MWCNTs increased a little from 1 wt.% to 5 wt.%, but decreased dramatically with PCS concentration in the range of 10–30 wt.%. The oxidation resistance of the coated MWCNTs was greatly improved in comparison with as-received ones. The oxidation peak temperature of the coated MWCNTs reached 783.7 °C, much higher than 652.2 °C for as-received ones.

Keywords: MWCNTs; SiC_xO_y coating; PCS; Oxidation resistance

1. Introduction

Since MWCNTs were discovered in 1991, they have attracted considerable attention due to their mechanical, chemical and physical properties, which makes them potentially useful in many applications in materials science, energy storage and energy conversion devices, hydrogen storage media, nanometer sized semiconductor devices and so on [1–3]. In the materials science field, much progresses have been made since MWCNTs were used as reinforcement to enhance the strength and toughness of ceramic and metallic matrix composites [4–9]. However, MWCNTs are easily oxidized in air and corroded after reacting with metals such as aluminum and iron, which has greatly restricted the wide application of MWCNTs. So far, chemical vapor deposition (CVD) has been successfully employed to deposit SiC coating on the surface of MWCNTs to improve their oxidation and corrosion resistance. However, this method, based on relatively complicated and time-consuming producers, is not always practical and cost-efficient. Furthermore, MWCNTs could easily transform into SiC nanorods and lose their superior properties if the reaction atmosphere was not well controlled [10–14].

PCS as a very important ceramic precursor, was widely used for the preparation of SiC coatings on the carbon materials to improve their oxidation resistance [15,16]. However, few papers have been published dealing with fabrication of ceramic coating on the surface of MWCNTs using PCS as precursor. By studying pyrolysis properties of PCS, Quanly et al. and Shimoo et al. showed that pyrolysis atmosphere and temperature had obvious influence on the final products of PCS [17–19]. For example, pyrolysis of PCS in vacuum could promote a more effective crystallization of the final products in comparison with a flow argon atmosphere. However, nearly all the reported papers focused on the pyrolysis of PCS in the flow argon or vacuum atmosphere. Pyrolysis of PCS in a coke bed which is a main sintering atmosphere of carbon-containing refractories, has never been reported before. Meanwhile, effect of PCS concentration on the thickness of the coating and oxidation resistance of the resulting samples has rarely been studied.

The present work, firstly, focuses on the study of pyrolysis products of PCS in a coke bed at different temperature such as 1000 °C, 1300 °C and 1500 °C. Based on the first part, it secondly tries to fabricate ceramic coating on the surface of MWCNTs using PCS as precursor and make out the effect of

* Corresponding author. Tel.: +86 27 68862188; fax: +86 27 68862018.
E-mail address: luoming19850302@126.com (M. Luo).

0272-8842/$36.00
doi:10.1016/j.ceramint.2011.05.033

PCS concentration on the oxidation resistance of the coated MWCNTs.

2. Experimental

2.1. Pyrolysis of PCS

Commercial PCS powder was used as precursor to generate ceramic products. Oxidative cross-linking (curing) of PCS was carried out by heating about 5 g PCS in an alumina crucible at 200 °C for 2 h in air. Pyrolysis of the cured PCS was carried out as follows. Firstly, the crucible with cured sample was covered with an alumina lid and then put in the middle position of an alumina sagger fed with carbon black. Subsequently, the sagger was heated in the electric furnace from room temperature to 1000 °C, 1300 °C and 1500 °C at a rate of 4 °C/min, respectively (Fig. 1). The dwell time at the final temperatures was 3 h. After the experiment, the sagger cooled down naturally in the furnace to room temperature.

2.2. Treatment of MWCNTs

For the preparation of ceramic coated MWCNTs, PCS solutions were firstly prepared by dissolving PCS powder into xylene. The PCS concentration in the solutions were 1 wt.%, 5 wt.%, 10 wt.%, 15 wt.% and 30 wt.%, respectively. Then MWCNTs (Alpha Nano Tech. Inc., Chengdu, China, diameter, 20–70 nm; length, ~20 μm; purity, >mass 95%; ash, <mass 1.5%) and the solutions with the ratio of 10 g/L were added into breakers and stirred homogeneously for 5 min, then ultrasonicated for 0.5 h. Subsequently, the solutions were removed under vacuum filtration and the residual samples were dried at 200 °C for 2 h in air. Lastly, the dried samples were pyrolyzed in the same experimental setup as the cured PCS from room temperature to 1500 °C using a heating rate of 4 °C/min and a holding time of 3 h.

2.3. Test and characterization methods

The phases composition of the pyrolyzed PCS as well as the treated MWCNTs were analyzed by X-ray diffraction (XRD, x'Pert Pro, Philips, Netherlands). Fourier transform infrared spectroscopy (FT-IR, Nicolet Avatar FT-IR 360, USA) spectra was obtained over the range of 4000–400 cm^{-1} using KBr discs to characterize the cured and pyrolyzed PCS. The surface morphology and microstructure of the pyrolyzed PCS powder, as well as as-received and treated MWCNTs were characterized by Raman spectroscopy (LabRam I, Dilor, France), scanning electron microscopy (SEM, Quanta 400, FEI Company, USA) equipped with energy dispersive X-ray spectroscopy (EDS, Noran 623M-3SUT, Thermo Electron Corporation, Japan) and high-resolution transmission electron microscope (HRTEM, 2000F, Jeol Ltd., Japan). Thermogravimetry-differential scanning calorimetry (TG-DSC, STA449, NETZSCH, Germany) was employed to analyze the pyrolysis process of the cured PCS in a flow argon atmosphere and oxidation resistance of the as-received and treated MWCNTs in a static air.

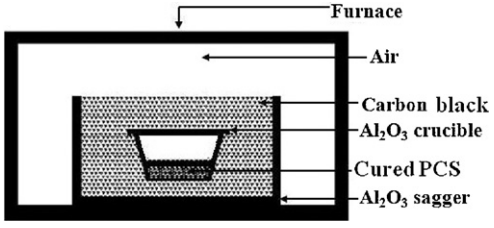

Fig. 1. Illustration of the experimental setup.

3. Results and discussions

3.1. Pyrolysis of PCS

The TG trace of the cured PCS in a flow argon atmosphere at a heating rate of 10 °C/min is shown in Fig. 2. The results indicated that the PCS had weight loss of about 40% between 100 °C and 1400 °C during the pyrolysis process. The weight loss could be divided into three stages [20]. The sharp loss for the first stage before 600 °C was associated with evaporation of the generated CH_4, H_2 and some small molecules via reactions (1) and (2). From 600 °C to 800 °C, the weight loss in the second stage should be due to the decomposition of organic side groups through the removal of excess carbon and formation of metastable SiC_xO_y ceramic. Above 800 °C, the conversion from polymer to ceramics was complete and decomposition of the SiC_xO_y ceramic with evaporation of gaseous SiO (g) and CO (g) accounted for the weight loss in the final stage via reaction (3).

$$\equiv Si - H + H - Si \equiv \rightarrow \equiv Si - Si \equiv + H_2 \quad (1)$$

$$2 \equiv Si - H + CH_3 - Si \equiv Si - H \rightarrow 2 \equiv Si - Si \equiv + CH_4 + H_2 \quad (2)$$

$$2SiC_xO_y(s) \rightarrow (1 + x - y)SiC(s) + (x + y - 1)CO(g) + (1 - x + y)SiO(g) \quad (3)$$

FT-IR spectras of the cured and pyrolyzed PCS are illustrated in Fig. 3. The deformation bands of H_2O from KBr were observed at 3400 cm^{-1} and 1620 cm^{-1} both for the cured and pyrolyzed PCS. As for cured PCS, the absorptions

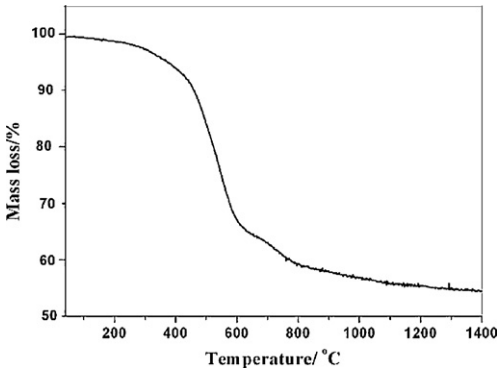

Fig. 2. TG curve of pyrolysis of the cured PCS in flow argon atmosphere.

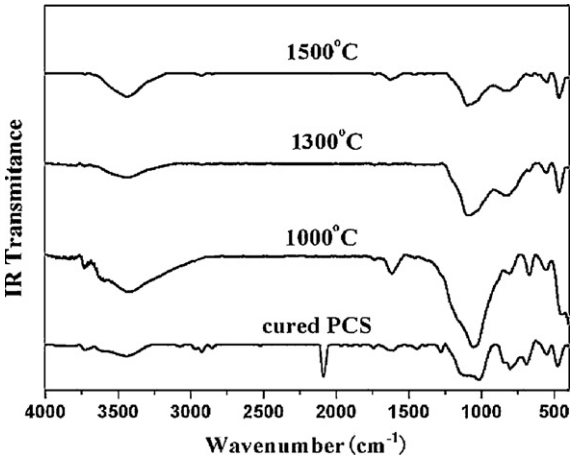

Fig. 3. FT-IR spectras of the cured and pyrolyzed PCS.

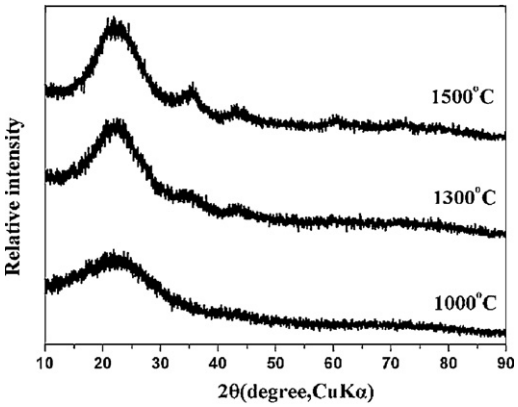

Fig. 4. XRD patterns of the pyrolyzed PCS.

around 1250 cm^{-1} and 2950 cm^{-1} were attributed to the stretching vibrations of Si–C and C–H stretching in Si–CH_3, respectively. The peak at about 2100 cm^{-1} was due to Si–H stretching. And the peaks at around 1050 cm^{-1} and 2920 cm^{-1} corresponded to C–H_2 bending and C–H stretching in Si–CH_2–Si. The other peaks at around 1030 cm^{-1} and 470 cm^{-1} were indicative of Si–O stretching and 1710 cm^{-1} of C=O stretching, which suggested that in the process of oxidation curing, the Si–H and Si–CH_3 groups of PCS were attacked by oxygen, creating Si–O and C=O bonds via reactions (4) and (5) [21]. After the cured PCS was pyrolyzed at 1000 °C, 1300 °C and 1500 °C, the spectral profile was typical of inorganic materials, where practically no absorption corresponding to organic groups from polymeric network was detected in comparison with the cured PCS. The spectra for the pyrolyzed PCS showed bonds at about 1600 and 800 cm^{-1}, associated to C–C and Si–C, as well as 1080 and 470 cm^{-1} to Si–O absorptions, respectively. The intensity of Si–C bond increased and Si–O bonds decreased with the increase of temperature, indicating that Si–O bonds gradually transformed into Si–C bond during the pyrolysis process.

$$2 \equiv Si - H + O_2 \rightarrow 2Si - OH \rightarrow \equiv Si - O - Si \equiv + H_2O \quad (4)$$

$$\equiv Si - CH_3 + O_2 \rightarrow \equiv Si - CH = O + H_2O \quad (5)$$

The XRD patterns of the cured PCS treated in the temperature range from 1000 °C to 1500 °C are shown in Fig. 4. As the treated temperatures increased, the broad halos from 22° to 24° (2θ) corresponding to amorphous SiC_xO_y and SiO_2 crystals became more concentrated, indicating that more SiO_2 crystals were formed [22]. Meanwhile, the low and broad diffractions peaks at 35.6°, 41.4°, 60.0°associated with (1 1 1), (2 0 0) and (2 2 0) planes of β-SiC crystals, appeared when PCS was treated at 1300 °C [19]. With the increase of temperature to 1500 °C, the diffractions peaks of β-SiC were more sharp and intensive, in agreement with better SiC crystallization and bigger β-SiC crystal size. In relation to the pyrolysis properties of PCS, it was reported by the previous paper that when PCS was pyrolyzed in flow argon or vacuum atmosphere, decomposition of amorphous SiC_xO_y to β-SiC and SiO_2 became complete with temperature up to 1300 °C [17]. However, the results were of great difference in the present work, which might be closely associated with the pyrolysis atmosphere. In a coke bed, the composition of atmosphere in the sagger were 3.5×10^4 Pa CO (g) and 6.5×10^4 Pa N_2 (g) in theory. In fact, a low partial pressure of O_2 (g) was still existed. By studying the effect of oxygen on the pyrolysis products of PCS, Kaneko et al. confirmed that introduction of oxygen into the PCS precursor could inhibit the formation of Si–C bonding (SiC crystallization) at elevated pyrolysis temperature, which leaded to the formation of stable Si–O bonding as Si–C–O (SiC_xO_y) forms [23]. Similar results were also observed by Shimoo et al. who used reduced pressure to pyrolyze PCS-derived SiC fibers [18]. So in this work it is deduced that, the relatively much higher O_2 (g) partial pressure in a coke bed compared with that contained in flow argon or vacuum atmosphere, might greatly hinder reaction (3) and inhibit the decomposition of SiC_xO_y, thus affecting crystallization of final products. On the other hand, high partial pressure of CO (g) in a coke bed might also cause damage to the crystallization of final products by decreasing equilibrium rate of reaction (3).

FESEM micrograph as well as EDS analyses of the powder obtained from the pyrolyzed PCS at 1500 °C is shown in Fig. 5. It is obvious that the vitreous grains as well as many balls with several micrometers in diameter coexisted with each other. Besides these, a small amount of nano-whiskers were embedded in the balls and others were located on the surface of vitreous grains. According to XRD and EDS analyses, such whiskers were β-SiC. Also, EDS analysis showed that the grains were composed of Si, O and C elements, in agreement with SiC_xO_y ceramic. However, only presence of Si and O elements in the EDS analysis confirmed that the balls were SiO_2. The results here confirmed the previous FT-IR and XRD analyses. Formation of SiC nano-whiskers could be explained by the reaction between SiO (g) and CO (g) via equation (6). Meanwhile, SiO_2 balls might be attributed to the oxidation of SiO (g) via reaction (7).

$$SiO(g) + 3CO(g) \rightarrow SiC(s) + 2CO_2(g) \quad (6)$$

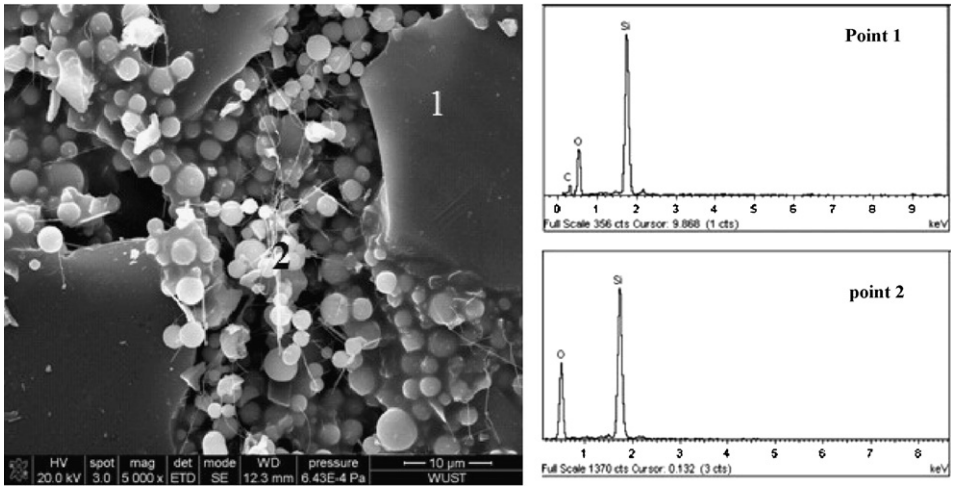

Fig. 5. FESEM micrograph and EDS analyses of the pyrolyzed PCS at 1500 °C.

$$2SiO(g) + O_2(g) \rightarrow 2SiO_2(s) \quad (7)$$

3.2. Formation of SiC_xO_y coating on MWCNTs

As discussed above, the pyrolysis products of PCS were composed of SiC_xO_y as the main phase, and SiC together with SiO_2 as the minor phase whose content had only a little increase as the treated temperature increased. Because of a little change of phase composition, 1500 °C as the pyrolysis temperature, was used to fabricate ceramic coating on the surface of MWCNTs. XRD patterns of the as-received and treated MWCNTs are shown in Fig. 6. The diffraction peaks at 26° were involved in (0 0 2) plane of the graphite structure of MWCNTs for all the samples. A small shoulder at 22–24°assigned to amorphous SiC_xO_y and a low peak at 35.6° accorded with β-SiC when PCS concentration was 5 wt.%. With the increase of PCS concentration to 30 wt.%, the amount of SiC_xO_y increased a lot, as well as a little increase of β-SiC. By adding 1 wt.% MWCNTs into Si–O–C ceramic, Segatelli et al. found that MWCNTs could promote a more effective crystallization of the SiC by reduction reaction between MWCNTs and SiC_xO_y above 1300 °C [19]. This work also coincides with the results because the SiC peak here was much sharper than the pyrolysis products of the cured PCS. But the reaction may be not noticeable in our work compared to their work, which may be probably due to the different systems and pyrolysis atmosphere as discussed above.

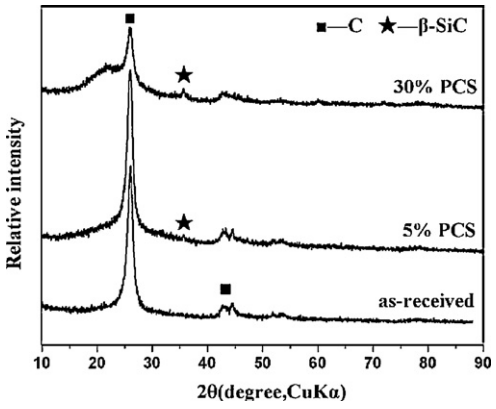

Fig. 6. XRD patterns of the as-received MWCNTs and MWCNTs treated with 5 wt.% and 30 wt.% PCS.

SEM micrographs of the as-received and treated MWCNTs are shown in Fig. 7. The diameter and length of as-received MWCNTs were 20–70 nm and 20 μm in average, respectively. Because of their high length-to-diameter ratio and low surface energy, MWCNTs were typically curved and entangled with each other. However, besides curved MWCNTs, some net-like structures and grains were also observed for treated MWCNTs, especially for MWCNTs treated with higher PCS concentration. When MWCNTs were treated with 1 wt.% PCS, the morphology did not change much compared with as-received ones. For 5 wt.% PCS, some SiC_xO_y grains knitting into net-like structures homogeneously dispersed and tangled MWCNTs together. With the increase to 10 wt.% PCS, some isolated balls as well as some grains detached from the MWCNTs. Combined with EDS analysis and the earlier discussion, the balls were SiO_2. Furthermore, the amount of isolated grains increased evidently and detached from MWCNTs when the PCS concentration reached 15 wt.%. Only the heads of some MWCNTs were exposed from the grains, while other MWCNTs located on the surface of the grains with the further increase of PCS concentration to 30 wt.%.

HRTEM micrographs of MWCNTs treated with 1 wt.%, 5 wt.% and 10 wt.% PCS are shown in Fig. 8. A coating was clearly observed on the surface of MWCNTs. The thickness of the coating for MWCNTs treated with 1% PCS was about 5–10 nm, and increased a little for 5% PCS. Higher magnification micrographs as well as the presence of Si, O and C elements in the EDS analysis (not shown), indicated that the coating was amorphous SiC_xO_y. HRTEM analysis could not detect the location of β-SiC phase although it was confirmed by the XRD analysis, which could be explained by its small amount. With the further increase of PCS concentration to 10 wt.%, the thickness of the coating decreased dramatically. The thickness

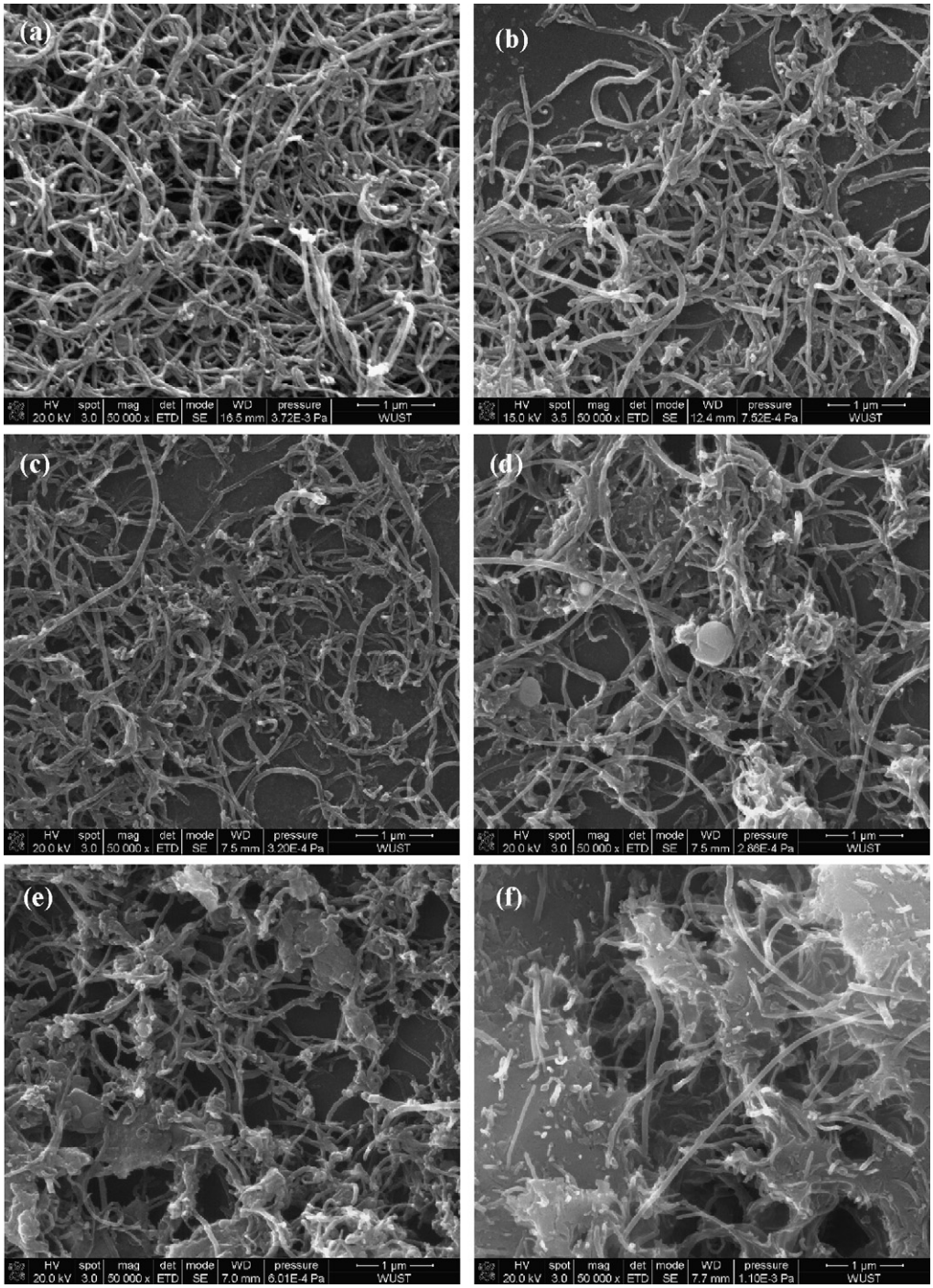

Fig. 7. SEM micrographs of the as-received MWCNTs (a) and MWCNTs treated with 1 wt.% (b), 5 wt.% (c), 10 wt.% (d), 15 wt.% (e) and 30 wt.% (f) PCS.

of the coating was closely related to the adsorption of PCS molecules on the surfaces of MWCNTs in the ultrasonicated process [24]. Under a certain PCS concentration, adsorption of PCS on the surfaces of MWCNTs improved with the increase of PCS concentration. However, over this concentration, the cohesive force between PCS molecules increased obviously. Once the cohesive force exceeded absorption force between PCS molecules and MWCNTs, PCS molecules were inclined to tangle together instead of absorbing on MWCNTs. As a consequence, absorption of PCS molecules on MWCNTs reduced and the thickness of the SiC_xO_y coating decreased accordingly. Therefore, more isolated SiC_xO_y grains were formed, but detached from the surface of MWCNTs, which was also confirmed by SEM analysis earlier. From the results above, it was obvious that 1–5 wt.% PCS concentration was more suitable for the absorption of PCS on MWCNTs and formation of SiC_xO_y coating.

In order to make out whether the structure of MWCNTs changed or not after treated, the Raman spectrums of the as-received MWCNTs and MWCNTs treated with 5 wt.% PCS are

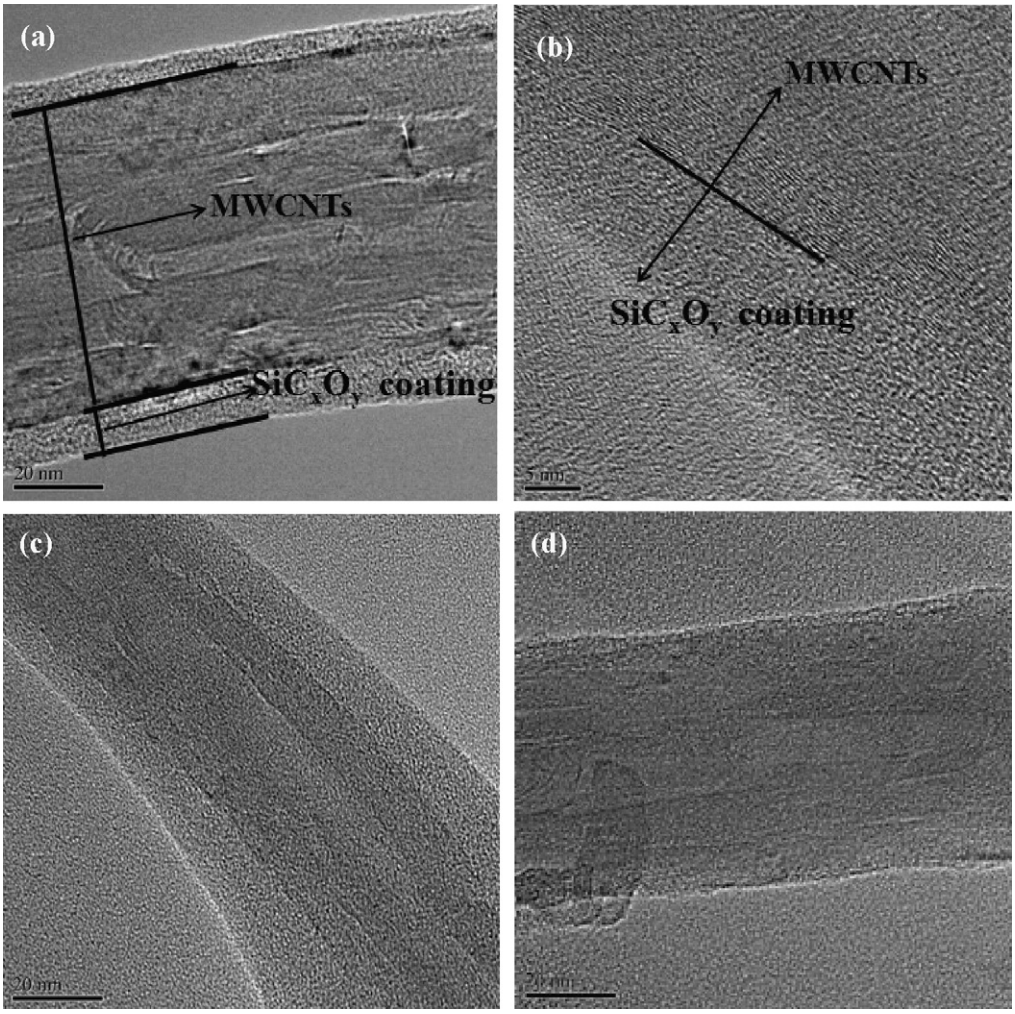

Fig. 8. HRTEM micrographs of MWCNTs treated with 1 wt.% (a)–(b), 5 wt.% (c) and 10 wt.% (d) PCS.

shown in Fig. 9. As for as-received MWCNTs, the relatively broad and low peak appeared at the wavenumber of about 1350 cm^{-1} (D-band) corresponded to disordered structure of amorphous carbon in the MWCNTs. And the sharp peak at 1575 cm^{-1} (G-band) was related to the graphite structure of MWCNTs. When MWCNTs were treated with 5 wt.% PCS, the intensity of D-band became a little higher, which was attributed to formation of a little amount of free carbon by pyrolysis of PCS [22]. But the graphite structure of the treated MWCNTs remained the same compared with as-received ones, indicating that the coating process did not change the structure of MWCNTs. Meanwhile, it was not surprising to observe SiC_xO_y peaks in the treated MWCNTs because of its much lower sensitivity in the Raman analysis.

3.3. Oxidation resistance of the coated MWCNTs

The oxidation resistance of all the treated MWCNTs including as-received ones was evaluated by TG-DSC measurement (Fig. 10). The samples were heated from room temperature to 1000 °C in a static air atmosphere at a rate of 10 °C/min. According to DSC curves (Fig. 10a), it was obvious that the starting temperatures (T_s), peak temperatures (T_p) and terminating temperatures (T_t) of the exothermic peaks for the treated MWCNTs were much higher than those of as-received MWCNTs (Table 1), demonstrating that the oxidation of MWCNTs was delayed and the oxidation resistance was greatly improved. It was not surprising to find that the oxidation resistance of the treated MWCNTs deteriorated with the

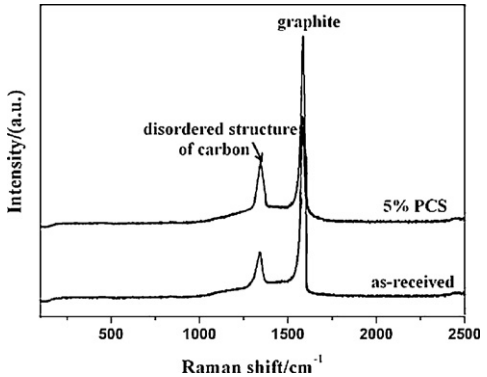

Fig. 9. Raman spectrums of the as-received MWCNTs and MWCNTs treated with 5 wt.% PCS.

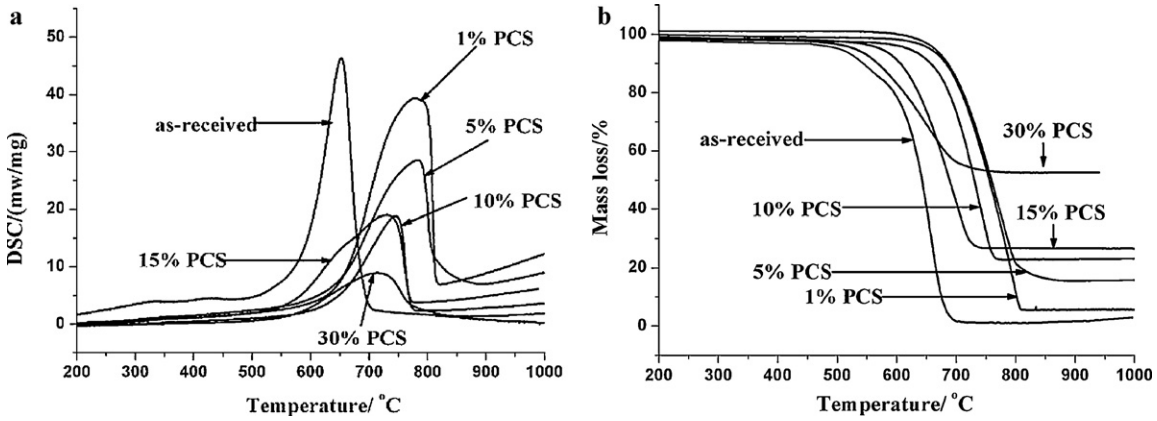

Fig. 10. DSC (a) and TG (b) curves of the as-received and treated MWCNTs.

Table 1
Characteristic temperatures of exothermic peaks of the as-received and treated MWCNTs.

Temperatures (°C)	As-received	After treated with different PCS concentration				
		1 wt.%	5 wt.%	10 wt.%	15 wt.%	30 wt.%
T_s	587.3	654.3	643.5	641.6	632.2	570.4
T_p	652.2	780.0	783.7	746.8	735.4	715.4
T_t	693.1	811.8	810.8	769.4	770.5	781.7

increase of PCS concentration from 10 wt.% to 30 wt.%, which was in agreement with the thickness of the coating on the surface of MWCNTs. The peak temperature for MWCNTs with 1 wt.% PCS was 780.0 °C, and increased a little when 5 wt.% PCS was used. However, it decreased evidently with the further increase of PCS concentration in the range from 10 wt.% to 30 wt.%. In addition, with the increase of PCS concentration, the height of the exothermic peaks declined and reached a minimum value at 30 wt.%, indicating that the content of MWCNTs in the samples decreased as more SiC_xO_y formed accordingly. Meanwhile, TG curves of all the samples measured during heating-up are presented in Fig. 10b. The mass loss at the end of the measurement was lower for the samples with higher PCS concentration, associated with the larger amount of SiC_xO_y ceramic.

4. Conclusions

SiC_xO_y ceramic was successfully coated on the surface of MWCNTs when PCS was used as precursor and pyrolyzed in a coke bed at 1500 °C. Pyrolysis products of PCS were composed of amorphous SiC_xO_y as main phase, together with β-SiC nanocrystals and SiO_2 crystals as the minor phases. The thickness of the coating increased a little from 1 wt.% to 5 wt.%, but decreased with the further increase of PCS concentration from 10 wt.% to 30 wt.%. The oxidation resistance of the treated MWCNTs improved greatly compared with the as-received ones. The oxidation peak temperature of the treated MWCNTs in a static air atmosphere reached 783.7 °C, higher than 652.2 °C for as-received ones.

Acknowledgements

This work is financially supported by Natural Science Foundation of Hubei Province (2009CDA050 and 2008CDB258), the New Century Excellent Talents in University (NCET-10-0137) and Natural Science Foundation of China (51072143).

References

[1] M.M.J. Treacy, T.W. Ebbesen, J.M. Gibson, Exceptionally high young's modulus observed for individual carbon nanotube, Nature 381 (1996) 678–680.
[2] M.F. Yu, O. Lourie, M.J. Dyer, K. Moloni, T.F. Kelly, Strength and breaking mechanism of multiwalled carbon nanotubes under tensile load, Science 287 (2000) 637–640.
[3] R.H. Baughman, A.A. Zakhidov, W.A. DeHeer, Carbon nanotubes-the route toward application, Science 297 (2002) 787–792.
[4] A. Kaleem, W. Pan, Effect of multi-walled carbon nanotube on mechanical properties and electrical conductivity of alumina, Rare Met. Mater. Eng. 36 (2007) 704–706.
[5] Y. Morisada, Y. Miyamoto, Y. Takaura, K. Hirota, N. Tamari, Mechanical properties of SiC composites incorporating SiC-coated multi-walled carbon nanotubes, Int. J. Refract. Met. Hard. Mater. 25 (2006) 322–327.
[6] J. Wang, H.M. Kou, X.J. Liu, Y.B. Pan, J.K. Guo, Reinforcement of mullite matrix with multi-walled carbon nanotubes, Ceram. Int. 33 (2007) 719–722.
[7] M. Estili, A. Kawasaki, An approach to mass-producing individually alumina-decorated multi-walled carbon nanotubes with optimized and controlled compositions, Scripta Mater. 58 (2008) 906–909.
[8] Y.F. Zhu, L. Shi, J. Liang, D. Hui, K.T. Lau, Synthesis of zirconia nanoparticles on carbon nanotubes and their potential for enhancing the fracture toughness of alumina ceramics, Composites 39 (2008) 1136–1141.
[9] G. Yamamoto, M. Omori, T. Hashida, H. Kimura, A novel structure for carbon nanotube reinforced alumina composites with improved mechanical properties, Nanotechnology 19 (2008) 1–7.
[10] H.J. Quah, K.Y. Cheong, Z. Lockman, Stimulation of silicon carbide nanotubes formation using different ratios of carbon nanotubes to silicon dioxide nanopowders, J. Alloys Compd. 475 (2009) 565–568.

[11] T. Taguchi, N. Igawa, H. Yamamoto, S.I. Shamoto, S. itsukawa, Preparation and characterization of single-phase SiC nanotubes and C-SiC coaxial nanotubes, Physica E 28 (2005) 431–438.
[12] B.S. Li, R.B. Wu, Y. Pan, L.L. Wu, G.Y. Yang, J.J. Chen, Simultaneous growth of SiC nanowires, SiC nanotubes, and SiC/SiO_2 core–shell nanocables, J. Alloys Compd. 462 (2008) 446–451.
[13] Y. Morisada, M. Maeda, T. Shibayanagi, Y. Miyamoto, Oxidation resistance of multiwalled carbon nanotubes coated with silicon carbide, J. Am. Ceram. Soc. 87 (2004) 804–808.
[14] Y. Morisada, Y. Miyamoto, SiC-coated carbon nanotubes and their application as reinforcements for cemented carbides, Mater. Sci. Eng. 381 (2004) 57–61.
[15] Z.Q. Fu, C.H. Tang, T.X. Liang, Structure of SiC coating from polycarbosilane on graphite for fuel element matrix of high temperature gas-cooled reactor, Surf. Coat. Technol. 200 (2006) 3950–3954.
[16] R.Q. Yao, Z.D. Feng, Y.X. Yu, S.W. Li, L.F. Chen, Y. Zhang, Synthesis and characterization of continuous freestanding silicon carbide films with polycarbosilane (PCS), J. Eur. Cream. Soc. 29 (2009) 2079–2085.
[17] H. Quanly, R. Taylor, R.J. Day, Conversion of polycarbosilane (PCS) to SiC-based ceramic PartII. Pyrolysis and characterization, J. Mater. Sci. 36 (2001) 4045–4047.
[18] T. Shimoo, K. Okamura, Effect of reduced pressure on oxidation and thermal stability of polycarbosilane-derived SiC fibers, J. Mater. Sci. 38 (2003) 4973–4979.
[19] M.G. Segatelli, E. Radovanovic, A.T.N. Pires, M.D.C. Goncalves, I.V.P. Yoshida, Influence of multiwall carbon nanotubes on the structural and morphological features of Si–C–O ceramics derived from a hybrid polymeric precursor, Mater. Chem. Phys. 2–3 (2010) 1216–1224.
[20] H.B. Li, L.T. Zhang, L.F. Cheng, Y.G. Wang, Z.J. Yu, M.H. Huang, Polymer–ceramic conversion of a highly branched liquid polycarbosilane for SiC-based ceramics, J. Mater. Sci. 43 (2008) 2806–3281.
[21] H. Wang, X.D. Li, X.X. Li, B. Zhu, D.P. Kim, The kinetics of oxidation of polycarbosilane fibers, Korean J. Chem. Eng. 21 (2004) 901–904.
[22] M.G. Segatelli, A.T.N. Pires, I.V.P. Yoshida, Synthesis and structural characterization of carbon-rich SiC_xO_y derived from a Ni-containing hybrid polymer, J. Eur. Cream. Soc. 28 (2008) 2247–2257.
[23] K. Kaneko, K.I. Kakimoto, HRTEM and ELNES analysis of polycarbosilane-derived Si–C–O bulk ceramics, J. Non-Cryst. Solids 270 (2000) 181–190.
[24] T.X. Liang, H.S. Zhao, X. Zhang, Electromagnetic wave absorption properties of SiC coated CNTs nano-composites, J. Inorg. Mater. 21 (2006) 559–563.